Chemical Engineering Journal 160 (2010) 267–276

Contents lists available at ScienceDirect

Chemical Engineering Journal

journal homepage: www.elsevier.com/locate/cej

Determination of the local micromixing structure in laminar flows

Edward P.L. Roberts*

School of Chemical Engineering and Analytical Science, University of Manchester, PO Box 88, Sackville St., Manchester M60 1QD, United Kingdom

ARTICLE INFO

Article history:
Received 6 August 2009
Received in revised form 27 February 2010
Accepted 1 March 2010

Keywords:
Micromixing
Lamellar modelling
Chaotic advection
Stretching
Backtracking

ABSTRACT

In rapidly mixing flows with low diffusion rates and/or fast reactions, accurate calculation of the local concentration distribution becomes impractical. One approach is to consider mixing segregated fluids and follow the interface between the two fluids as it stretches in the flow. For a rapid mixing flow such as a chaotic or turbulent flow, the area of the interface between segregated fluids grows exponentially, so that determination of the location of the interface rapidly becomes unfeasible. In this study, a method for calculating the local lamellar structure (i.e. the orientation and thicknesses of the lamellae) for any advection time and at any location in the flow is developed for two-dimensional flows. Locally the lamellar structure is assumed to be one-dimensional, and the orientation of the lamellae can be determined from the direction corresponding to the maximum stretching rate for fluid arriving at the location. The lamellar structure can be readily determined by mapping a short finite line, oriented perpendicular to the orientation of the lamellae, backwards in time to the initial conditions. Once the line is returned to its initial location the intersection of the line with the initial interface between the segregated fluids can be used to accurately determine the detailed lamellar structure, in particular the thicknesses of the lamellae. The accuracy of the method is demonstrated for two deterministic chaotic flows, the sine flow and a piecewise linear flow, the saw-tooth flow. The use of the piecewise linear flow enables accurate testing of the method as precise simulations of the full interface can be obtained for relatively long advection times, where the initial interface is a polygon.

1. Introduction

For flows with slow diffusion or fast reaction, the simulation of mixing processes is an important and challenging problem. Such processes include combustion [1], fast and mixing sensitive reactions [2] and reaction injection moulding of polymers [3]. While increasingly complex flows are becoming accessible to numerical simulation using Eulerian computational fluid dynamics, accurate simulation of mixing and reaction processes continues to be an important challenge. For fast mixing flows, the length scale of the concentration field rapidly becomes smaller than practical grid sizes leading to numerical diffusion errors.

If we consider mixing segregated fluids in the absence of diffusion, the mixing process is described by the location of the interface between the fluids. For a fast mixing flow such as a chaotic or turbulent flow, this interface stretches at an exponential rate [4–6]. The consequence of this exponential stretching rate for mixing simulations is that the data storage capacity required to describe the interface rapidly becomes excessive. Ottino [5] and others [7] have suggested that the mixing rate can be characterised by the stretching rate of infinitesimal lines advected by the flow. The distribution of this stretching rate can be plotted across the flow field to illustrate the mixing distribution or averaged for optimisation studies [7,8]. While this approach can be useful, it fails to describe the complete mixing process and the link to processes with diffusion and reaction is unclear. In addition, it has been shown [9] that the stretching of the interface is not a useful measure for comparing the mixing achieved under different conditions. In terms of the mixing characteristics proposed by Dankwerts [10], interface stretching is also not useful for predicting the intensity of segregation.

In spite of the issue of exponential stretching rates, significant progress has been made in describing the mixing process, particularly in two-dimensional chaotic flows. A widely used approach has been to consider diffusion and reaction processes occurring in layers of segregated fluid in a lamellar structure [11–20]. Studies of mixing in these flows [21–23] have shown that after a short time, a one-dimensional lamellar structure is formed locally, with all lamellae oriented in the same direction. In Dankwerts terms, the characteristic thickness of the lamellae corresponds to a mixing measure: the scale of segregation [10]. In the absence of diffusion, the mixing at any location can be described simply by the thicknesses of the lamellae. For processes with diffusion and reaction, one-dimensional simulations within these lamellar structures, including the effects of stretching, are relatively straightforward [11,15,18,24].

* Tel.: +44 0 161 306 8849; fax: +44 0 161 306 9321.
E-mail address: edward.roberts@manchester.ac.uk.

1385-8947/$ – see front matter © 2010 Elsevier B.V. All rights reserved.
doi:10.1016/j.cej.2010.03.001

Muzzio and co-workers [23] have shown that for chaotic flows the local lamellar structure is oriented in the direction of maximum stretching rate, which is parallel to the unstable manifold for a chaotic flow. They termed this property '*asymptotic directionality*'. Furthermore, they have shown that the distribution of the lamellar thicknesses (in particular the probability density function – PDF) can be accurately estimated from the distribution of stretching rates in the flow. In addition, Clifford et al. [18] showed that the volume averaged stretch rate can be used with a very simple one-dimensional model to describe the progress of a reaction in a chaotic flow.

However, for mixing sensitive reactions, studies have shown that the reaction yield can depend strongly on the order that lamellae are arranged [19]. Cox [25] has also shown that lamellar models fail to accurately follow mixing and reaction processes as they do not include a description of how the detailed micromixing structure develops with time. It is normally assumed that the detailed local microstructure can only be obtained by following the full interface between segregated fluids. However, for long mixing times this presents significant difficulties. In rapid mixing flows the interface stretches exponentially, so that memory required to describe the interface becomes very large. Moreover, it has previously been shown [26] that the error ε in the calculation of lamellae thicknesses associated with using a chain of points to describe the interface is of order:

$$\varepsilon \sim \left(\frac{d^2}{8Rw}\right) \tag{1}$$

where d is the separation of the points, R is the radius of curvature of the interface and w is the thickness of the lamellar. As w decreases at an exponential rate, not only is the length of the interface increasing but the spacing between the points required to describe the interface is also decreasing. For rapidly mixing flows, calculation of the full lamellar structure is widely considered to be impractical for significant mixing time.

In this paper we develop an alternative method for the calculation of the local lamellae structure, without the need to follow the interface between segregated fluids. The focus is on two-dimensional deterministic flows, but the methods developed may be generalised to other types of flow.

2. Determination of local lamellar structure

To date, the only reported method for determining the local lamellar structure at some location $(\boldsymbol{X}, \tau)$ formed by the passive advection of a segregated fluid in a chaotic flow is to accurately follow the interface (a material line $\boldsymbol{\Gamma}$) surrounding the segregated fluid [6]. The local lamellar thicknesses can then be found by determining the intersection points between a short line oriented perpendicular to the lamellae. The location of the interface after advection time τ, $\boldsymbol{\Gamma}_\tau$, is normally determined by advecting a chain of passive points arranged along the interface [6,27], ensuring that the spacing between points remains small by adding points to the original interface $\boldsymbol{\Gamma}_0$.

Here we take a new approach by considering the advection backwards in time of a finite line $\boldsymbol{\gamma}_\tau$, oriented perpendicular to the lamellae (see Fig. 1). The orientation of the line can be readily determined as the local lamellae will be oriented in the direction of maximum stretching $\boldsymbol{s}$ for a point arriving at $(\boldsymbol{X}, \tau)$. For a two-dimensional chaotic flow this corresponds to the direction of the positive local Liapunov exponent at $(\boldsymbol{X}, \tau)$. The perpendicular direction corresponds to the direction of minimum stretching, which is negative (i.e. the direction of the negative local Liapunov exponent). If we consider advection backwards in time from $(\boldsymbol{X}, \tau)$ to $(\boldsymbol{X}_0, 0)$, the stretching rates are inverted: the direction of minimum (negative) stretching for the forward advection becomes the direction of maximum (positive) stretching for the reverse advection (backwards in time). The finite line thus stretches rapidly in the reverse flow. We can now examine the location of this finite line after it has been advected and stretched back to $t = 0$, $\boldsymbol{\gamma}_0$ (Fig. 1). The location of intersection points ($\boldsymbol{Y}_{i,0}$) between the line $\boldsymbol{\gamma}_0$ and the initial boundary of the segregated fluid $\boldsymbol{\Gamma}_0$ correspond to the edges of the lamellae in the vicinity of $(\boldsymbol{X}, \tau)$. The thicknesses of the lamellae can be thus be found by determining the length of the line at $t = 0$ between adjacent intersection points ($\boldsymbol{Y}_{i,0}$ and $\boldsymbol{Y}_{i+1,0}$) and the average stretching rate between the points (experienced as the line is advected back from $t = \tau$ to $t = 0$). Note that the method is not effective at locations where the interface has high curvature, usually corresponding to folds in the lamellar structure. However, in rapid mixing flows this is unlikely to occur, and it would be relatively easy to check the curvature at the location.

We can thus formulate a procedure for determining the local lamellar structure at around any location $(\boldsymbol{X}, \tau)$, which we will call the '*backtracking method*':

(i) Advect the location $(\boldsymbol{X}, \tau)$ backwards in time to $(\boldsymbol{X}_0, 0)$, determine the deformation tensor T for this motion and the associated direction of maximum stretching.

(ii) Advect a finite length line $\boldsymbol{\gamma}_\tau$, centred at $\boldsymbol{X}$ and oriented in the direction of maximum stretching for the motion from $(\boldsymbol{X}, \tau)$ to $(\boldsymbol{X}_0, 0)$. The line can be followed by advecting a chain of points $\boldsymbol{P}_{i,\tau}$ backwards in time to $\boldsymbol{P}_{i,0}$, and adding points to the original line $\boldsymbol{\gamma}_\tau$ if the distance between adjacent points exceeds a suitable tolerance Δ.

(iii) At each point $\boldsymbol{P}_i$ in the chain of points used to describe the line, determine the local stretching s_i of the line experienced during the advection backwards in time from $t = \tau$ to $t = 0$. This stretching can be determined by following the advection of a vector $\delta\boldsymbol{P}_{i,\tau}$ applied at $\boldsymbol{P}_i$, and the stretching s_i is defined as

$$s_i = \frac{\left\| \delta \boldsymbol{P}_{i,0} \right\|}{\left\| \delta \boldsymbol{P}_{i,\tau} \right\|}. \tag{2}$$

(iv) Determine the location of intersection points $\boldsymbol{Y}_{i,0}$ between the line $\boldsymbol{\gamma}_0$ and the boundary of the initial segregated region of fluid $\boldsymbol{\Gamma}_0$.

(v) To find the thickness of the lamella between $\boldsymbol{Y}_{i,\tau}$ and $\boldsymbol{Y}_{i+1,\tau}$, we account for the shrinking (s^{-1}) of the line $\boldsymbol{\gamma}_0$ as it is advected forward to $\boldsymbol{\gamma}_\tau$:

$$w_i = \int_{Y_{i,\tau}}^{Y_{i+1,\tau}} s^{-1} \mathrm{d}\boldsymbol{\gamma}_\tau. \tag{3}$$

In principle this method can be applied to any two-dimensional flow where passive points can be advected forward or backwards in time. In this study we use simple periodic deterministic flows which exhibit a high degree of chaos in the advection behaviour in order to test the described above. The lamellae thicknesses at some location in the flow are determined firstly by following the boundary $\boldsymbol{\Gamma}$ between the segregated fluids and secondly by the backtracking method proposed above. The deterministic flows used for this study are described in the subsequent section.

3. Deterministic flows

Simple deterministic flows which exhibit chaotic advection have been widely studied since Aref demonstrated chaotic behaviour in a two-dimensional periodic journal bearing flow [28]. We have selected two highly idealised flows to use as a test bed for the method described in the previous section. The first of these is the sine flow (SF), as under suitable conditions this exhibits

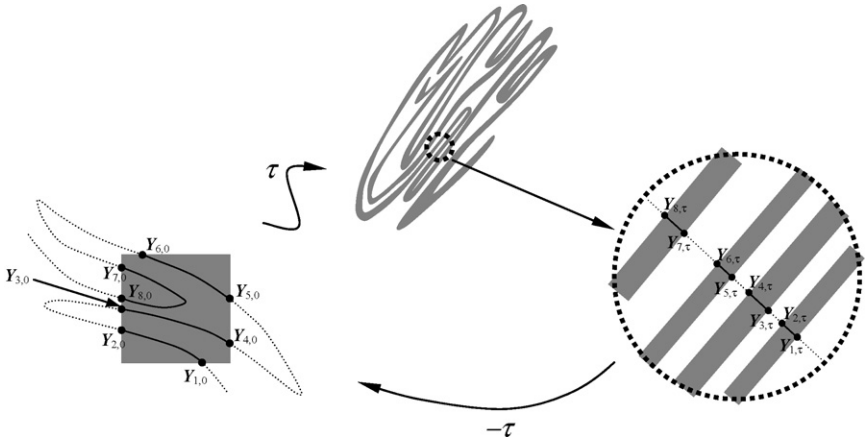

Fig. 1. Schematic illustration of the advection of a segregated region of fluid forwards and backwards in time. A finite line perpendicular to the local lamellar structure advected backwards in time will stretch to intersect the initial segregated region at points corresponding to the edges of the lamellae.

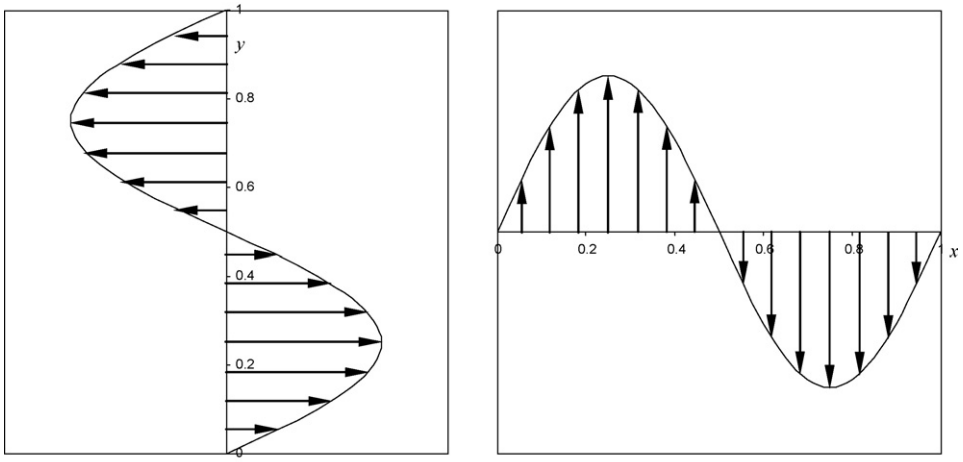

Fig. 2. Periodic velocity field for the sine flow, (a) $nT \le t < (n+(1/2))T$ and (b) $(n+(1/2))T \le t < nT$.

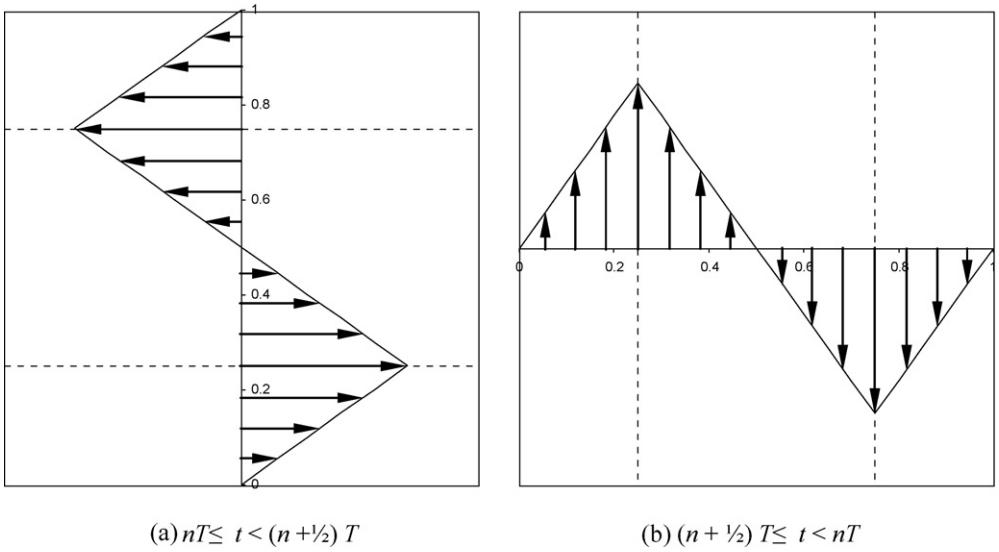

Fig. 3. Periodic velocity field for the saw-tooth flow, (a) $nT \le t < (n+(1/2))T$; and (b) $(n+(1/2))T \le t < nT$. The dashed lines indicate the shear planes corresponding to discontinuities in the velocity gradient.

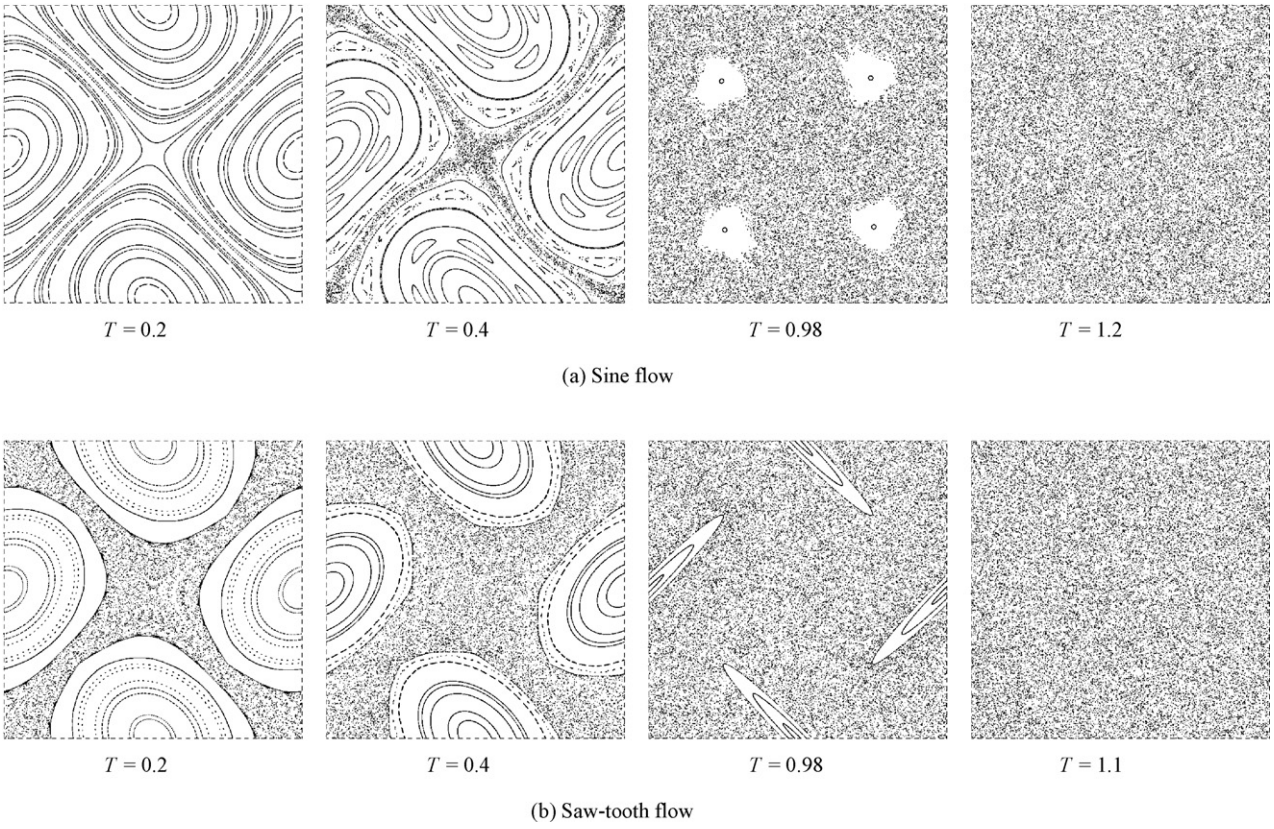

Fig. 4. Poincaré maps for (a) sine flow and (b) saw-tooth flow at a range of flow periods T. The periodic velocity fields are defined in Eqs. (3) and (4) (sine flow) and (5)–(10) (saw-tooth flow).

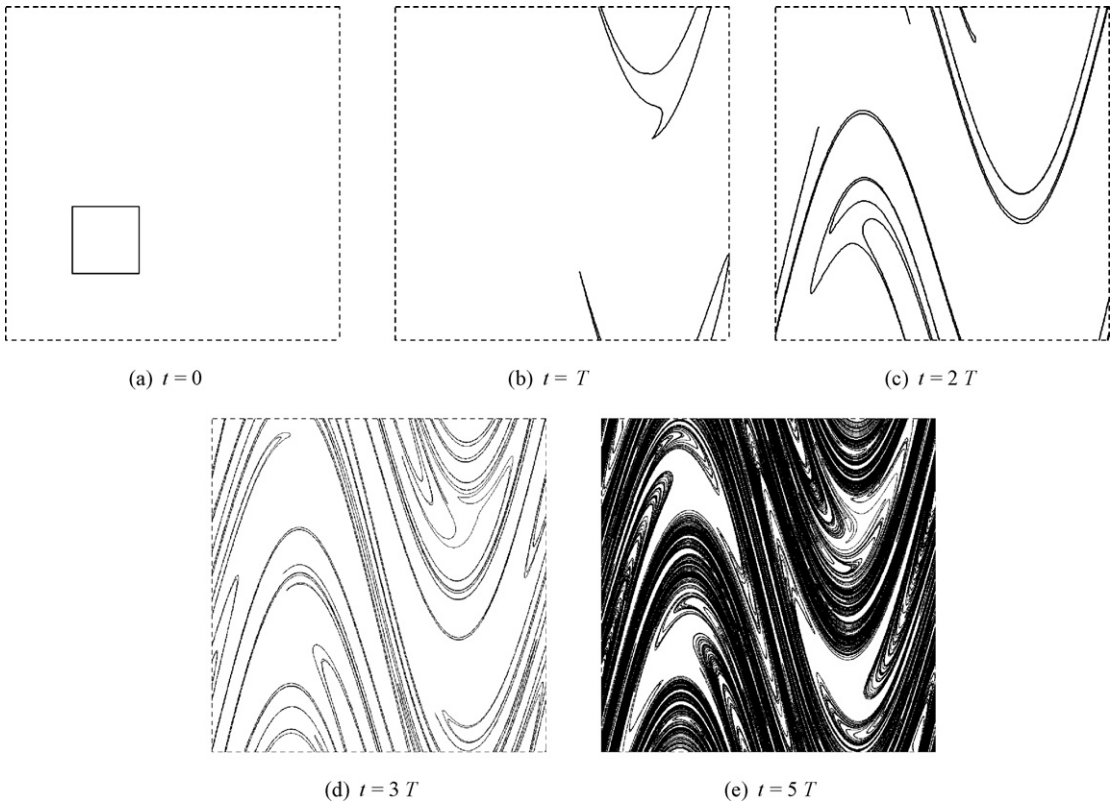

Fig. 5. Advection of a passive boundary for five cycles of the sine flow with a flow period of $T = 1.2$, (a) $t = 0$; (b) $t = T$; (c) $t = 2T$; (d) $t = 3T$; and (e) $t = 5T$.

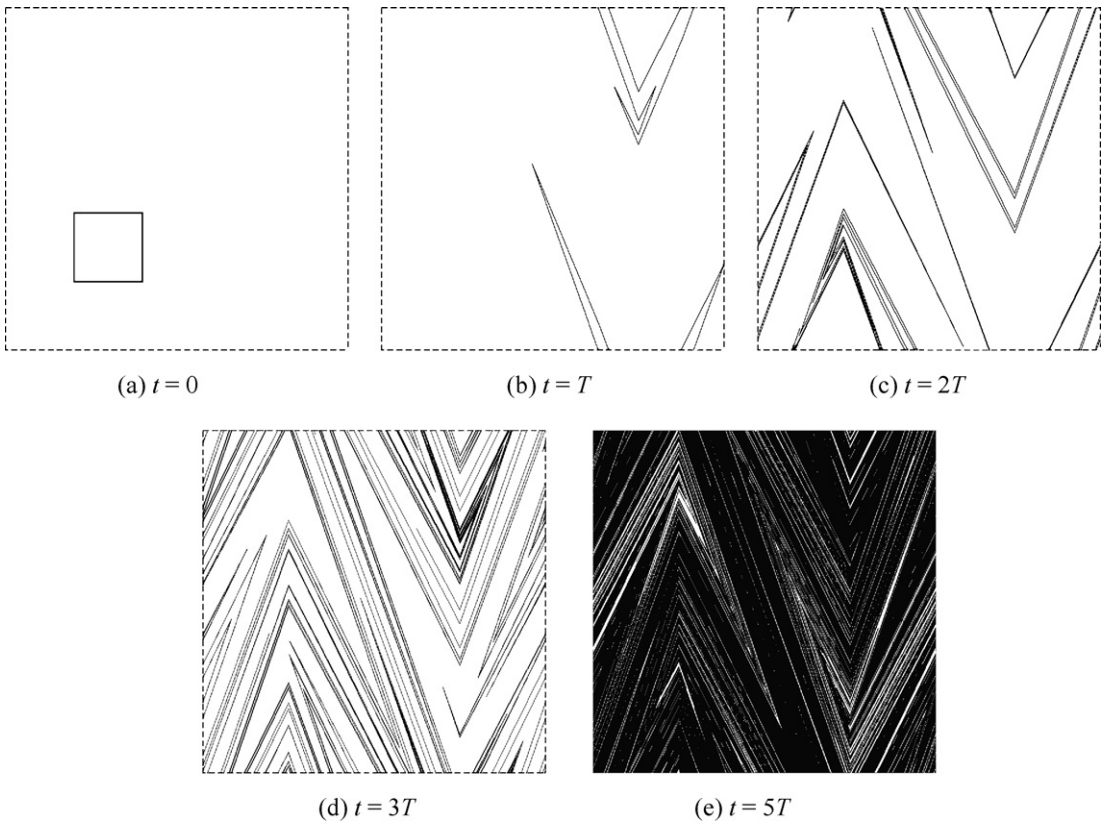

Fig. 6. Advection of a passive boundary for five cycles of the saw-tooth flow with a flow period of $T = 1.2$, (a) $t = 0$; (b) $t = T$; (c) $t = 2T$; (d) $t = 3T$; and (e) $t = 5T$.

strong chaotic mixing and has been widely used for mixing studies [6,18,23,27,29]. The sine flow is spatially and temporally periodic, with the velocity field defined as follows:

$$\boldsymbol{v} = (\sin\ 2\pi y, 0), \qquad nT \le t < \left(n + \frac{1}{2}\right) T, \tag{4}$$

$$\boldsymbol{v} = (0, \sin 2\pi x), \qquad \left(n + \frac{1}{2}\right) T \le t < (n+1)T \tag{5}$$

where x and y are dimensionless coordinates, T is the flow period, n is the number of periods and t is the time. This flow field is illustrated in Fig. 2.

As discussed in the introduction, accurate determination of lamellae thicknesses by following the boundary $\boldsymbol{\Gamma}$ between segregated fluids is a significant challenge. Since we wish to test an alternative method, we have used a piecewise linear flow similar to the sine flow, which enables more accurate determination of the lamellae thicknesses from the boundary for the case where $\boldsymbol{\Gamma}_0$ is a polygon with straight sides. This flow, first described by Pasmanter [30], is very similar to the sine flow, but uses a saw-tooth wave rather than a sine wave for the velocity fields (Fig. 3):

$$nT \le t < \left(n + \frac{1}{2}\right) T:$$

$$\boldsymbol{v} = (4y, 0), \qquad 0 \le y < \frac{1}{4}, \tag{6}$$

$$\boldsymbol{v} = (2 - 4y, 0), \qquad \frac{1}{4} \le y < \frac{3}{4}, \tag{7}$$

$$\boldsymbol{v} = (4y - 4, 0), \qquad \frac{3}{4} \le y < 1, \tag{8}$$

$$\left(n + \frac{1}{2}\right) T \le t < nT:$$

$$\boldsymbol{v} = (0, 4x), \qquad 0 \le x < \frac{1}{4}, \tag{9}$$

$$\boldsymbol{v} = (0, 2 - 4x), \qquad \frac{1}{4} \le x < \frac{3}{4}, \tag{10}$$

$$\boldsymbol{v} = (0, 4x - 4), \qquad \frac{3}{4} \le x < 1, \tag{11}$$

The mixing behaviour of these two flows depends strongly on the flow period T, with islands of order observed associated with elliptic periodic points for $T < \sim 1.1$. Poincaré maps for the sine flow and the saw-tooth flow are shown in Fig. 4 for a range of values of T. These were obtained by advecting 100 passive markers distributed evenly in the unit box ($0 \le x \le 1, 0 \le y \le 1$) and plotting their location after each cycle of motion ($t = T, 2T, 3T, \ldots$) for 300 cycles. For these maps the spatial periodic boundary conditions were used so that when a particle flowed out of the box it immediately re-entered on the opposite side.

In both cases stationary elliptic points occur at the centre of each side of the unit box, with associated islands of order at low values of T. At the centre of the unit box there is a hyperbolic stationary point. Chaotic regions grow around this hyperbolic point as the flow period is increased, and these are generally larger for the saw-tooth flow than the sine flow at the same flow period. As T approaches 1, four islands of order appear in the sine flow associated with period two elliptic points. In both cases the chaotic regions appear to fill the flow field at large T.

4. Local lamellar structure

For each flow the local lamellar structure has been determined by two methods for globally chaotic flows ($T = 1.2$ for the sine flow and $T = 1.1$ for the saw-tooth flow). The first method, which we will call the *boundary method*, is the conventional method of follow-

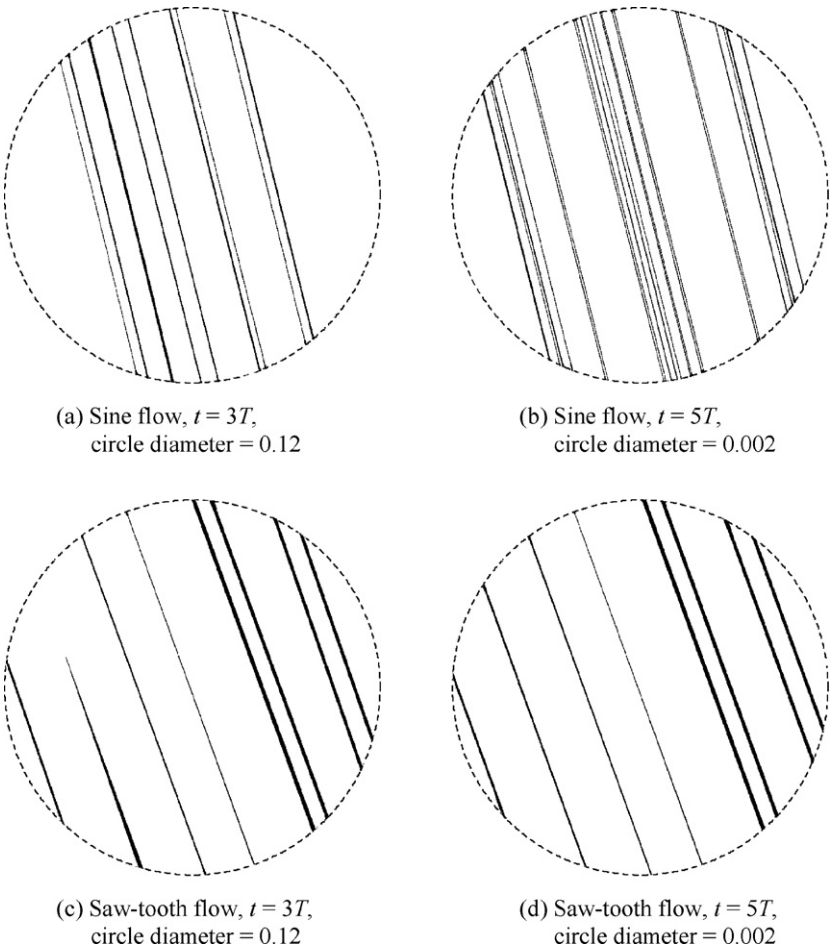

Fig. 7. Lamellae structure formed in the sine and saw-tooth flows at the location $X = (0.5, 0.5)$, for $T = 1.2$, (a) sine flow, $t = 3T$, circle diameter = 0.12; (b) sine flow, $t = 5T$, circle diameter = 0.002; (c) saw-tooth flow, $t = 3T$, circle diameter = 0.12; and (d) saw-tooth flow, $t = 5T$, circle diameter = 0.002. The black regions indicate fluid that was inside the segregated region of fluid shown in Fig. 4(a) at $t = 0$.

ing the boundary $\mathbf{\Gamma}$ of the segregated fluid. Initially the segregated region of fluid is a square box with sides of length 0.2 and centred at (0.3, 0.3) as shown in Fig. 5(a). As the boundary stretches in the sine flow points are added to the original boundary $\mathbf{\Gamma}_0$ to ensure that no two points on $\mathbf{\Gamma}_t$ are separated by a distance of more than $\Delta = 0.005$. Fig. 5 shows the location of the boundary after one, two, three and five cycles for $T = 1.2$. In order to maximise the number of lamellae obtained at any location, periodic boundary conditions were used as before. This is equivalent to there being an equivalent segregated region of fluid in all adjacent unit boxes (i.e. for all $i \le x \le i+1, j \le y \le j+1$, where i and j are integers). The boundary stretches rapidly so that after a few cycles the structure of the segregated fluid within the unit box becomes almost indistinguishable, appearing to fill most of the box.

In the case of the saw-tooth flow, it is not necessary to add points to the original boundary. The linear nature of the flow ensures that

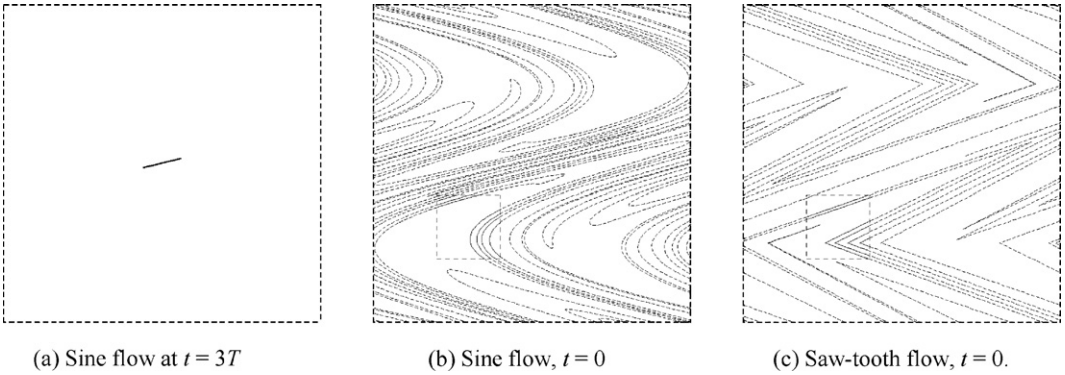

Fig. 8. Location of a finite line across the lamellae (a) at $X = (0.5, 0.5)$, $t = 3T$, and after advection backwards in time to $t = 0$ for the (b) sine and (c) saw-tooth flow, $T = 1.2$. Note that the line in (a) is for the sine flow; for the saw-tooth flow the orientation of the line is slightly different. At $t = 0$ the line is a dashed line except where it intercepts the square segregated region, corresponding to lamellae at X, $t = 3T$.

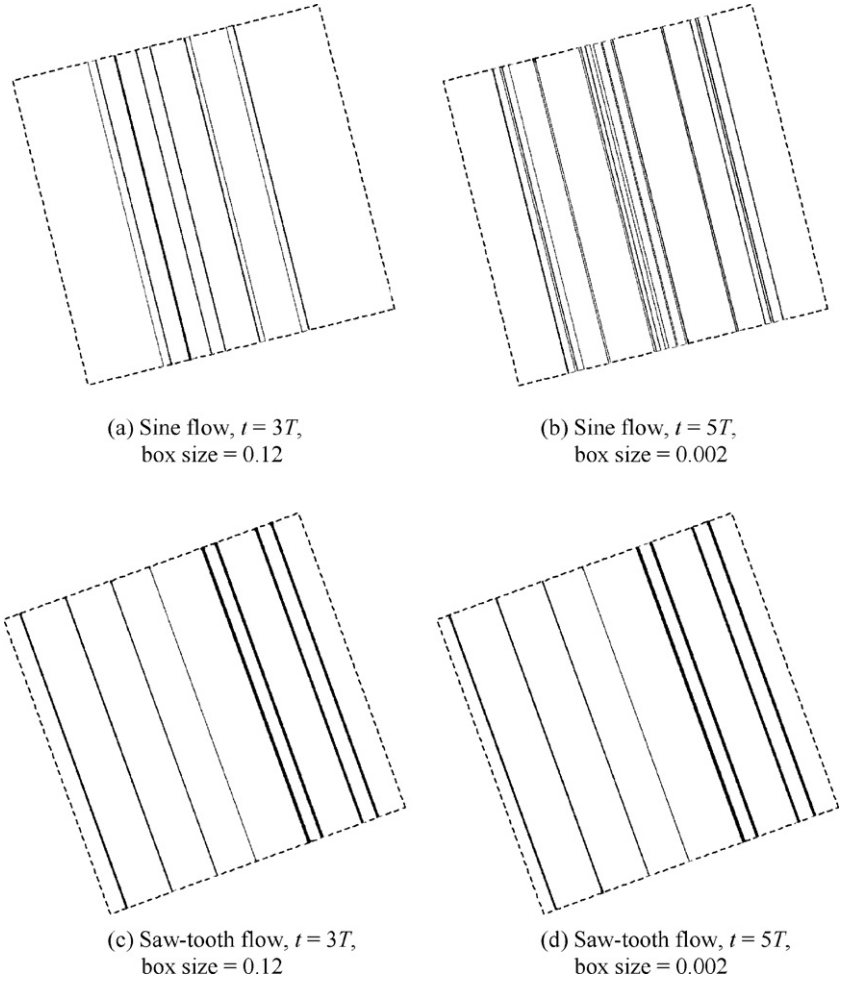

Fig. 9. Lamellar structure at $X = (0.5, 0.5)$ for $T = 1.2$, determined by the backtracking method described in the text, (a) sine flow, $t = 3T$, box size = 0.12; (b) sine flow, $t = 5T$, box size = 0.002; (c) saw-tooth flow, $t = 3T$, box size = 0.12; and (d) saw-tooth flow, $t = 5T$, box size = 0.002. The nine and eight lamellae shown in (a) and (c), respectively correspond to the intersections of the stretched finite line with the initial segregated fluid shown in Fig. 7 (b) and (c).

straight lines advected in the flow remain straight, and on each half cycle simply fold at the shear planes shown in Fig. 3:

$$t = nT, \qquad y = \frac{1}{2}i + \frac{1}{4} \tag{12}$$

$$t = \left(n + \frac{1}{2}\right)T, \quad x = \frac{1}{2}i + \frac{1}{4} \tag{13}$$

where n and i are integers. A polygon boundary $\mathbf{\Gamma}_0$ (such as a square box) advected in the flow thus remains a polygon with increasing numbers of sides. The boundary can be followed by simply adding vertices wherever the boundary crosses the shear planes defined by Eqs. (12) and (13) on each half cycle. For the range of flows studied the lengths of the sides of the polygon is of same order as the distance between the shear planes (0.5), so the number of points

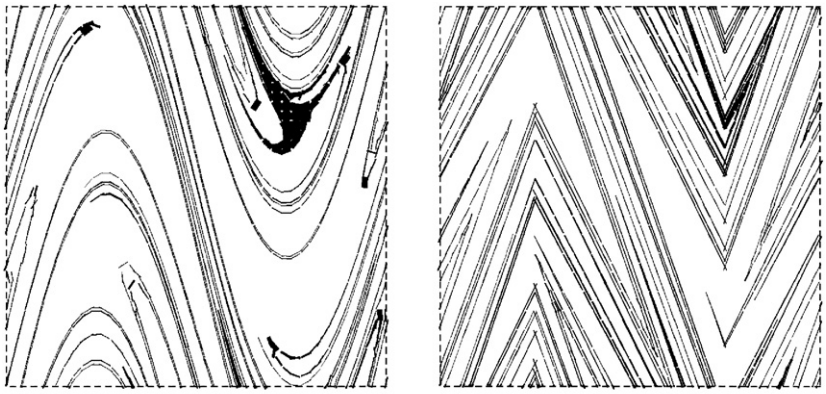

Fig. 10. Map of the lamellar structure across the unit box generated by stretching a finite line across the lamellae at each location backwards in time, as described in the text, for (a) the sine flow and (b) the saw-tooth flow with $T = 1.2$.

Table 1
The number of points required to describe the passive boundary for a segregated region of fluid as it is advected in the sine and saw-tooth flows.

t/T	Sine flow	Saw-tooth flow
1	1,214	6
2	9,293	28
3	60,620	152
4	377,237	914
5	2,239,229	5,284
6	11,716,088	30,234
7		173,660
8		996,894
9		5,718,624

required to follow the boundary is several orders of magnitude less that that for the sine flow or other two-dimensional chaotic flows that have been used in previous studies of this type. This is illustrated in Table 1, which compares the number of points required to describe the boundary for the sine flow and the saw-tooth flow over a series of six flow periods. The reduced memory requirement enables longer simulations to be performed with the saw-tooth flow. For example the number of points required exceeds 10^7 after between 5 and 6 cycles of the since flow at $T = 1.2$, and after between 9 and 10 cycles of the saw-tooth flow at the same flow period. While this does not seem particularly impressive, the length of interface is growing at an exponential rate. Thus with the saw-tooth flow it is possible to simulate a boundary that is more than 250 times longer than that achieved for the sine flow, using the same number of data points.

In addition to the reduced data required, the boundary is completely defined by the location of the vertices, so that the thickness of the lamellae at any point can be accurately determined. For flows such as the sine flow which generate curved boundaries, this is not the case since the location of the boundary between points on the boundary must be approximated by interpolation. For very thin lamellae this can lead to significant error unless the separation between boundary points is very small, as indicated by Eq. (1). Eq. (1) further emphasises this difference, since for the saw-tooth flow where the interface is straight, there is no error in the determination of lamellae thicknesses associated with the description of the interface as a chain of points, since the radius of curvature of the interface, R, is infinite.

The saw-tooth flow is thus an excellent flow with which to evaluate the proposed method for determining the local lamellar structure. Fig. 6 shows the boundary location in the saw-tooth flow after one, two, three and five cycles for the saw-tooth flow with $T = 1.2$, using periodic boundary conditions as before. As with the sine flow, the boundary almost completely fills the unit box after five cycles.

We now consider the local lamellar structure at a point in the flow. For the purposes of this study, the location of the point is not important. The central point $X = (0.5, 0.5)$ has been chosen since a fine lamellar structure is formed at this location. This point also has the advantage that the radius of curvature for the sine flow is large, so that the error in the determination of lamellae thicknesses using the boundary method is low at this location. Fig. 7 shows the lamellar structure observed at this location after three and five cycles for the two flows, obtained from the boundary method, using the simulation of the boundary shown in Figs. 5 and 6. The length scale of the lamellar structure decreases with increasing time as expected. The orientation of the lamellae shown in Fig. 7 are perpendicular to the directions of maximum stretching for the advection from $\boldsymbol{X}$ to $\boldsymbol{X}_0$, which were found to be 0.0776 π and 0.1106 π radians (relative to the x direction) for the sine flow and saw-tooth flow, respectively.

Using the backtracking method described above this local lamellar structure can be determined by advecting a finite line $\boldsymbol{\gamma}_\tau$, centred at $X = (0.5, 0.5)$ and perpendicular to the orientation of maximum stretching, backwards in time. Fig. 8 shows the line $\boldsymbol{\gamma}_0$, after advection backwards in time for three cycles of the sine flow and saw-tooth flow. The line is shown as a dotted line in Fig. 8, except where it intersects with the location of the segregated region of fluid, where it is shown as a solid line. These solid lines correspond to the lamellae which are formed at $X = (0.5, 0.5)$ when the line is advected forwards in time. Thus for the sine flow the line intersects the segregated region nine times, indicating that there are nine lamellae within a circle of diameter 0.12 at ($\boldsymbol{X}$, 3T), consistent with Fig. 7(a). Similarly for the saw-tooth flow eight lamellae are expected to occur as observed in Fig. 7(c).

Fig. 9 shows the lamellae structure at $X = (0.5,0.5)$ after an advection time of 3T determined using the backtracking method. The thickness of each layer of fluid was determined by a numerical integration of Eq. (3). For the first layer the limits of the integration are the start of the line and the first point of intersection between the backtracked line (shown in Fig. 8) and the interface. For subsequent layers the limits are sequential intersection points between the backtracked line and the interface. The layers were then plotted as rectangular blocks with a thickness calculated from the numerical integration, length equal to the length of the perpendicular line before it is backtracked, and with the long side oriented in the direction of maximum stretching at $\boldsymbol{X}$. The layers were filled where the backtracked line fell inside the interface. The thicknesses

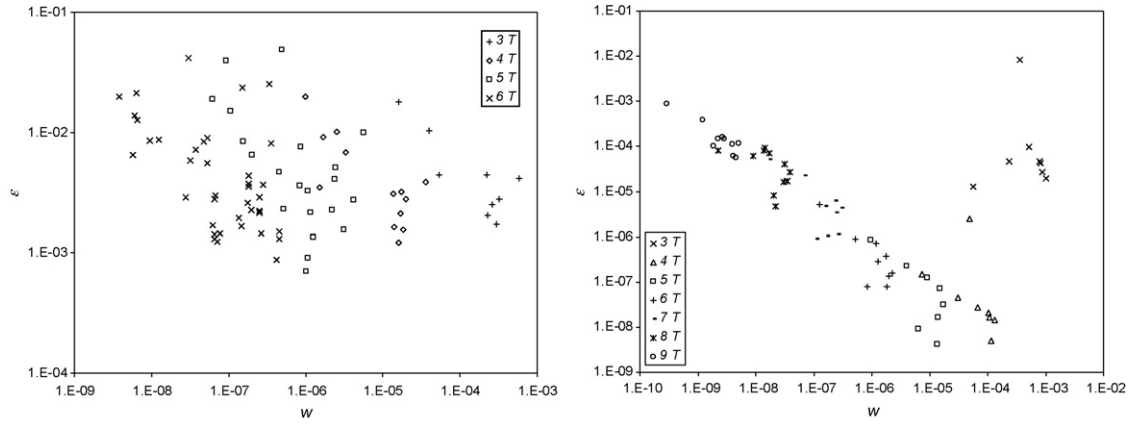

(a) Sine flow (b) Saw-tooth flow

Fig. 11. Normalised difference between the lamellar thicknesses at $X = (0.5, 0.5)$ determined from the advection of the passive boundary of a segregated region of fluid and by stretching a finite line at X across the lamellae backwards in time, as described in the text, for (a) the sine flow and (b) the saw-tooth flow with $T = 1.2$.

of the fluid layers originating from both inside and outside the segregated region must be calculated to determine the lamellar structure. There is close agreement between the lamellar structures observed in Figs. 7 and 9, for both the sine and saw-tooth flows.

Fig. 7(c) and 9(c) illustrate the weakness of the one-dimensional assumption, as the folding point [the end of the lamellar layer which does not span the circle in Fig. 7(c)], cannot be observed with the one-dimensional assumption used in the backtracking method. However, comparison of Figs. 7 and 9 gives a qualitative indication that the backtracking method can be used to determine the local lamellar structure without the need to follow the boundary of the segregated region. The qualitative comparison can be extended by constructing the lamellar structure across the entire unit cell. Fig. 10 shows the lamellar structure determined by the backtracking method at an array of 1600 locations distributed within the unit cell. Comparison with the simulations of the passive boundary in Figs. 5 and 6 confirms that the backtracking method is an effective method for determining the lamellar structure.

To obtain a more quantitative indication of the accuracy of the method, the difference between the lamellae thicknesses determined from the two methods was determined. Fig. 11 shows the variation of the normalised error ε:

$$\varepsilon = \frac{\left|w' - w\right|}{w} \tag{14}$$

where w and w' are the lamellar widths determined from the boundary and backtracking methods, respectively. For the sine flow [Fig. 11(a)] the difference is at most a few percent, even for the very thin lamellae obtained after six cycles. The error is caused by a combination of factors including the numerical integration in the backtracking method (Eq. (3)) and the error in the boundary method associated with the approximation of the passive boundary as a chain of points [26]. Note that the maximum distance between adjacent points on the boundary was 0.005 for advection times of $3T$ and $4T$, and 0.002 and 0.001 for $5T$ and $6T$, respectively.

With the saw-tooth flow the main sources of error are eliminated, as the location of the boundary is precisely defined by the vertices and the stretching is constant on each line segment, so there is no error in the numerical integration of Eq. (3). There is a small difference in the orientation used to measure the lamellar thicknesses, as for the boundary method this is based on the orientation of the boundary in the vicinity of $\boldsymbol{X}$, while for the backtracking method it is based on the orientation with maximum stretching at $\boldsymbol{X}$. However, the observed error is close to what would be expected from truncation errors, with the exception of the data for an advection time of $3T$. For this case the higher error is probably due to differences in the orientations used, as the one-dimensional approximation is less accurate at short advection times.

5. Conclusions

In this study we have shown that the local lamellar structure can be accurately determined without the need to simulate the boundary of the entire passive boundary of a segregated region of fluid. The method is efficient for determining the lamellar structure at a particular location or at an array of locations in a rapidly mixing flow. Although it has been shown that the structure throughout the mixture can be determined using the backtracking method, this uses a similar amount of computational effort as a full simulation of the interface, since the total length of the stretched array of backtracked lines will be similar or even longer than that of the full interface. However, the method is memory efficient as it is not necessary to store the information to describe the backtracked lines, merely the orientation and lamellae thicknesses at each location. In addition, by obtaining the micromixing structure at an array of locations, the method could be used to obtain statistical information on the lamellar structure for situations where full simulation is impractical. In this way it could be used to map the distribution of the micromixing structure in a mixing process and to construct new micromixing, diffusion and reaction models.

The method is suitable for flows for which the one-dimensional lamellar model can be used. However, the method does not require excessive memory and the numerical error can be controlled to ensure an accurate structure is obtained. The conventional simulation of the full boundary fails at long advection times as the memory requirement increases exponentially. Using the backtracking method, only the fluid around the location of interest is advected (backwards in time), so only relevant fluid is simulated. The method is not limited to short advection times and in principle could be used for arbitrary time. However, for rapid mixing systems for long advection times the length scale of the lamellar structure will become very fine and may require extended precision to eliminate truncation errors. In practice the length scale and hence the advection time will be limited by diffusion processes.

The one-dimensional assumption leads to errors associated with curvature of the boundary and lamellae. The curvature itself could be accommodated by determining the local radius of curvature which can be readily obtained [31,32]. However, the ends and folds of lamellae cannot be readily observed using the backtracking method. The folding of fluid in chaotic flows is an area that merits further study in relation to micromixing processes. A simple two-dimensional approach which could be used to describe the local lamellar structure would be to simulate the advection of an array of points around a location backwards in time and determine which of them originated in the segregated region. The accuracy of this method would be limited by the initial separation of adjacent points prior to their advection backwards in time.

The backtracking method could be readily combined with simulations of diffusion and reaction to improve the accuracy of micromixing simulations. The method has been tested for deterministic two-dimensional flows, but can be applied to any two-dimensional flow where a full description of the Eulerian flow field has been obtained. In principle, the method could be readily extended to three-dimensional flows provided the one-dimensional approximation can be applied. Practical applications include laminar flow processes including the oscillatory flow reactor [33], microfluidic devices [34] and static mixers [35]. Direct numerical simulations of turbulent flows also open the possibility of studying more complex systems such as combustion processes.

Another interesting possibility is to use the backtracking method for simulation of mixing of fluids with different properties (e.g. different viscosities). For short advection times full simulations could be used until this becomes unfeasible due to memory constraints or numerical errors. The backtracking method could then be used to determine the local fluid structure at longer times, from which the local fluid rheology could be determined.

References

[1] H. Pitsch, Large-eddy simulation of turbulent combustion, Annu. Rev. Fluid Mech. 38 (2006) 453–482.
[2] J.R. Bourne, F. Kozicki, P. Rys, Mixing and fast chemical-reaction. 1. Test reactions to determine segregation, Chem. Eng. Sci. 36 (1981) 1643–1648.
[3] R.J. Santos, A.M. Teixeira, J.C.B. Lopes, Study of mixing and chemical reaction in RIM, Chem. Eng. Sci. 60 (2005) 2381–2398.
[4] J.G. Franjione, J.M. Ottino, Feasibility of numerical tracking of material lines and surfaces in chaotic flows, Phys. Fluids 30 (1987) 3641–3643.
[5] J.M. Ottino, The Kinematics of Mixing, Cambridge University Press, Cambridge, 1989.
[6] S. Cerbelli, M.M. Alvarez, F.J. Muzzio, Prediction and quantification of micromixing intensities in laminar flows, AIChE J. 48 (2002) 686–700.
[7] E.P.L. Roberts, M.R. Mackley, The simulation of stretch rates for the quantitative prediction and mapping of mixing within a channel flow, Chem. Eng. Sci. 50 (1995) 3727–3746.
[8] E.P.L. Roberts, Unsteady Flow and Mixing in Baffled Channels, Department of Chemical Engineering, Cambridge University, Cambridge, 1992.

[9] O.S. Galaktionov, P.D. Anderson, G.W.M. Peters, H.E.H. Meijer, Morphology development in kenics static mixers (application of the extended mapping method), Can. J. Chem. Eng. 80 (2002) 604–613.
[10] P.V. Dankwerts, The definition and measurement of some characteristics of mixtures, Appl. Sci. Res. 3 (1952) 279–296.
[11] W.E. Ranz, Applications of a stretch model to mixing, diffusion, and reaction in laminar and turbulent flows, AIChE J. 25 (1979) 41–47.
[12] I.M. Sokolov, A. Blumen, Diffusion-controlled reactions in lamellar systems, Phys. Rev. A 43 (1991) 2714–2719.
[13] S.D. Fields, J.M. Ottino, Effect of segregation on the course of unpremixed polymerizations, AIChE J. 33 (1987) 959–975.
[14] S.D. Fields, J.M. Ottino, Effect of striation thickness distribution on the course of an unpremixed polymerization, Chem. Eng. Sci. 42 (1987) 459–465.
[15] F.J. Muzzio, J.M. Ottino, Dynamics of a lamellar system with diffusion and reaction—scaling analysis and global kinetics, Phys. Rev. A 40 (1989) 7182–7192.
[16] F.J. Muzzio, J.M. Ottino, Evolution of a lamellar system with diffusion and reaction—a scaling approach, Phys. Rev. Lett. 63 (1989) 47–50.
[17] F.J. Muzzio, J.M. Ottino, Diffusion and reaction in a lamellar system—self-similarity with finite rates of reaction, Phys. Rev. A 42 (1990) 5873–5884.
[18] M.J. Clifford, S.M. Cox, E.P.L. Roberts, Lamellar modelling of reaction, diffusion and mixing in a two-dimensional flow, Chem. Eng. J. 71 (1998) 49–56.
[19] M.J. Clifford, S.M. Cox, E.P.L. Roberts, Reaction and diffusion in a lamellar structure: the effect of the lamellar arrangement upon yield, Physica A 262 (1999) 294–306.
[20] S.M. Cox, M.J. Clifford, E.P.L. Roberts, A two-stage reaction with initially separated reactants, Physica A 256 (1998) 65–86.
[21] J.M. Ottino, Description of mixing with diffusion and reaction in terms of the concept of material-surfaces, J. Fluid Mech. 114 (1982) 83–103.
[22] J.M. Ottino, C.W. Leong, H. Rising, P.D. Swanson, Morphological structures produced by mixing in chaotic flows, Nature 333 (1988) 419–425.
[23] F.J. Muzzio, M.M. Alvarez, S. Cerbelli, M. Giona, A. Adrover, The intermaterial area density generated by time- and spatially periodic 2D chaotic flows, Chem. Eng. Sci. 55 (2000) 1497–1508.
[24] S.D. Fields, J.M. Ottino, Effect of stretching path on the course of polymerizations—applications to idealized unpremixed reactors, Chem. Eng. Sci. 42 (1987) 467–477.
[25] S.M. Cox, Chaotic mixing of a competitive-consecutive reaction, Physica D 199 (2004) 369–386.
[26] M.J. Clifford, S.M. Cox, E.P.L. Roberts, Measuring striation widths, Phys. Lett. A 260 (1999) 209–217.
[27] M.M. Alvarez, F.J. Muzzio, S. Cerbelli, A. Adrover, M. Giona, Self-similar spatiotemporal structure of intermaterial boundaries in chaotic flows, Phys. Rev. Lett. 81 (1998) 3395–3398.
[28] H. Aref, Stirring by chaotic advection, J. Fluid Mech. 143 (1984) 1–21.
[29] M. Liu, F.J. Muzzio, R.L. Peskin, Effects of manifolds and corner singularities on stretching in chaotic cavity flows, Chaos Soliton Fract. 4 (1994) 2145–2167.
[30] R.A. Pasmanter, Anomalous diffusion and anomalous stretching in vortical flows, Fluid Dyn. Res. 3 (1988) 320–326.
[31] I.T. Drummond, W. Munch, Distortion of line and surface elements in model turbulent flows, J. Fluid Mech. 225 (1991) 529–543.
[32] M. Liu, F.J. Muzzio, The curvature of material lines in chaotic cavity flows, Phys. Fluids 8 (1996) 75–83.
[33] T. Howes, M.R. Mackley, E.P.L. Roberts, The simulation of chaotic mixing and dispersion for periodic flows in baffled channels, Chem. Eng. Sci. 46 (1991) 1669–1677.
[34] D.S. Kim, S.W. Lee, T.H. Kwon, S.S. Lee, A barrier embedded chaotic micromixer, J. Micromech. Microeng. 14 (2004) 798–805.
[35] O.S. Galaktionov, P.D. Anderson, G.W.M. Peters, H.E.H. Meijer, Analysis and optimization of kenics static mixers, Int. Polym. Proc. 18 (2003) 138–150.